RESEARCH ARTICLE

Developing selective L-Amino Acid Transport 1 (LAT1) inhibitors: A Structure-Activity Relationship overview

Authors

Michael F. Wempe[1], Promsuk Jutabha[2], Vijay Kumar[1], James A. Fisher[4], Katie Waers[4], Meagan D. Holt[1], Andrew M. Dodson[1], Julia Bautista[1], Deshae T Gehr[1], Donald S. Backos[1], Amit Kumar[1], Peter J. Rice[4], Naohiko Anzai[3], Kunio Saito[5], Koji Oda[6], Yoshikatsu Kanai[7], and Hitoshi Endou[8]

Affiliations

[1]Department of Pharmaceutical Sciences, School of Pharmacy, University of Colorado Denver Anschutz Medical Campus, C238; 12850 E. Montview Blvd. Aurora, CO 80045, USA
[2]Chakri Naruebodindra Medical Institute, Faculty of Medicine Ramathibodi Hospital, Mahidol University, 111 Moo 4 Bang Pla, Bang Phli District, Samut Prakan 10540, Thailand
[3]Department of Pharmacology and Toxicology, Dokkyo Medical University School of Medicine, 880 Kitakobayashi, Mibu, Shimotsuga, Tochigi, 321-0293, Japan
[4]Department of Pharmacology, East Tennessee State University Johnson City, TN, 37614 USA
[5]Tanabe R&D Service Co., LTD. 2-2-50 Kawagishi, Toda-shi, Saitama 335-8505, Japan
[6]Yokohama Technical Support Group, Laboratory Animal Management Group, Tanabe R&D Service Co., LTD. 1000, Kamoshida-cho, Aoba-ku, Yokohama 227-0033, Japan
[7]Department of System Pharmacology, Osaka University School of Medicine, 2-2 Yamadaoka Suita, Osaka 565-0871 Japan
[8]Department of Pharmacology and Toxicology, Kyorin University School of Medicine, Mitaka, Tokyo, 181-8611 Japan

Corresponding Author:
Michael F. Wempe
Associate Research Professor, Department of Pharmaceutical Sciences, School of Pharmacy, University of Colorado Denver, C238 V20-2105 12850 East Montview Blvd. Aurora, CO 80045.
(Tel) 303-724-8982; (Fax) 303-724-7266
Michael.Wempe@cuanschutz.edu

Abbreviations:
Structure-Activity Relationship (SAR); L-type amino acid transporter 1 (LAT1).

ABSTRACT

System L amino acid transporters are a member of the Solute Carrier transporter Family (SLC). L-Amino acid transporter 1 (LAT1) belong to SLC7 and requires the heavy chained 4F2hc chaperone protein for amino acid transport. LAT1 is expressed in tumor cells and cancerous cells *in vivo* are strongly linked to LAT1 expression. Herein, we provide historical aspects regarding initial Structure Activity Relationship (SAR) findings reported in 2002 with the oocyte model and in 2008 with S2-LAT1 and S2-LAT2 cell lines. We summarize a series of dichloro- dibromo- and diiodo- tyrosine analogs that were prepared, and tested their potential to inhibit leucine transport in vitro to afford IC_{50} values with a few being low microM LAT1 inhibitors. We then summarize our efforts regarding novel LAT1 inhibitors with sub-nanomolar (nM) IC_{50}s to produce JPH203 which has completed Phase I clinical trial and is currently in Phase II trial in Japan. We describe differences observed between LAT1 and LAT2. Overall, we provide an expanded SAR model regarding potent and selective LAT1 inhibitors.

Introduction

A member of the Solute Carrier Transporter Family (SLC), System L includes L-Amino Acid Transporter 1 (LAT1), LAT2, LAT3, and LAT4. [1-4] LAT1 and LAT2 belong to SLC7, while LAT3 and LAT4 belong to SLC43. It is well established that LAT1 and LAT2 require the heavy chained 4F2hc chaperone protein for amino acid transport activity, whereas LAT3 and LAT4 do not. [5] LAT1 and LAT2 are hetero-dimeric large amino acid transporters expressed in various tissues and appear to act as 1:1 exchangers in concert with other amino acid transporters. LAT1 and LAT3 appear to be selectively expressed in tumor cells [3, 6]; consequently we regard these transporter proteins as potential oncology drug targets. In contrast to LAT1, LAT2's mRNA has low expression in tumor cells, but expressed with high frequency in normal tissues. [2] Furthermore, it has been shown that many primary human tumors and tumor cell lines (*e.g.* uterine cervical carcinoma cells (*i.e.* HeLa), bladder carcinoma cells (*i.e.* T24), and lung small-cell carcinoma cells (*i.e.* RERF-LC-MA) highly express LAT1. [6] In a rat liver metastases model, LAT1 expression correlated well with tumor cell growth. [7] LAT1 over-expression has also been reported in pulmonary adenocarcinoma and esophageal carcinoma. [8, 9] LAT1 expression was investigated in sixty patients with astrocytic brain tumors and statistical analysis illustrated that high LAT1 expression correlated with limited survival. [10] Furthermore, it was recently reported that LAT1 expression is a pathological factor that predicts the prognosis of non-small cell lung cancer (NSCLC) and prostate cancer. [11, 12] Hence, the experimental data demonstrate that cancerous and/or proliferating cells *in vivo* are strongly linked to LAT1 expression.

In 1998, LAT1 expression cloning was first reported and we initially probed LAT1's structure-activity relationship (SAR) by conducting experiments using rat LAT1 (rLAT1) and 4F2hc expressed in the *Xenopus laevis* oocyte system. [1] These data provided initial insight regarding LAT1 substrate recognition. [13] In those experiments, both uptake and efflux experiments were conducted using [^{14}C]phenyl-alanine **1** as a model substrate. Consistent with competitive inhibition, LAT1-mediated uptake was strongly inhibited by aromatic-amino acid derivatives such as L-dopa **2**, methyldopa **3**, melphalan **4**, triiodothyronine **5**, and thyroxine **6**. In contrast, phenylalanine methyl ester **7**, *N*-methyl phenylalanine **8**, dopamine **9**, tyramine **10**, carbidopa **11**, and droxidopa **12** did not inhibit [^{14}C]phenyl-alanine uptake (**Table 1**, oocyte data). These *in vitro* data supported the notion that small aromatic amino acids require the free carboxylic acid (*i.e.* non-ester) and amino group (*i.e.* no alkyl groups on the amine) in order to be an LAT1 substrate. [13] While the oocyte expression system was a useful and informative *in vitro* system, we sought to develop methods amendable for compound high throughput screening (HTS) and a system to study human (*i.e.* hLAT1 and hLAT2).

Table 1 LAT1 and LAT2 ^{14}C-Leu Uptake Inhibition Summary

Compound	R_1	R_2	R_3	R_4	R_5	R_6	R_7	hLAT1 μM	hLAT2 μM
1	CO_2H	NH_2	H	H	H	H	H	11	24
2	CO_2H	NH_2	H	H	OH	OH	H	(67)	NI
3	CO_2H	NH_2	H	H	OMe	OH	H	(56)	NI
4	CO_2H	NH_2	H	H	H	$N(CH_2CH_2Cl)_2$	H	(49)	NI
5	CO_2H	NH_2	H	H	I	O(3IPhOH)	I	(5.8)	NI
6	CO_2H	NH_2	H	H	I	O(3,5diIPhOH)	I	(90)	NI
7	CO_2Me	NH_2	H	H	H	H	H	NI	NI
8	CO_2H	NHMe	H	H	H	H	H	NI	NI
9	H	NH_2	H	H	OH	OH	H	NI	NI
10	H	NH_2	H	H	H	OH	H	NI	NI
11	CO_2H	$NHNH_2$	Me	H	OH	OH	H	NI	NI
12	CO_2H	NH_2	H	OH	OH	OH	H	NI	NI
13	CO_2H	H	NH_2	H	H	H	H	96	NI
14	CO_2H	NH_2	H	H	H	OH	H	(31) 20	41
15	CO_2H	NH_2	H	H	H	F	H	13	14
16	CO_2H	NH_2	Me	H	H	H	H	75	NI
17	CO_2H	NH_2	Me	H	H	OH	H	85	NI
18	CO_2H	NH_2	CH_2OH	H	H	OH	H	NI	NI
19	CO_2H	CH_2OH	NH_2	H	H	OH	H	NI	NI
20*	CO_2H	NH_2	H	H	F	H	F	23	72
21	CO_2H	NH_2	H	H	H	NO_2	H	131	61
22	CO_2H	NH_2	H	H	NO_2	OH	H	37	44
23	CO_2H	NH_2	H	H	I	OH	H	8.0	19
24	CO_2H	NH_2	H	H	I	OH	I	15	NI
25	CO_2H	NH_2	H	Ph	H	H	H	20	107
26	CO_2H	H	H	NH_2	H	O-Me	H	NI	NI
27	CH_2OH	NH_2	H	H	H	OH	H	NI	NI
28	CO_2H	NH_2	Me	H	F	OH	H	54	NI

NI = no inhibition at 150 microM

In 2008 we reported the establishment of a mammalian cell line expressing hLAT1 or hLAT2 [14]; we refer to these two cell lines as S2-hLAT1 and S2-hLAT2, respectively. These cell lines afford robust *in vitro* cell based tools to evaluate the interaction of known and novel compounds to chemically compare hLAT1 versus hLAT2. In this model, we use [^{14}C]L-leucine uptake to investigate the structural and inhibitory differences between hLAT1 and hLAT2. S2-hLAT1 cells are inhibited by L-isomers of leucine, isoleucine, valine, phenylalanine, tyrosine, tryptophan, methionine,

histidine, and a classical SL specific inhibitor, 2-aminobicyclo-(2,2,1)-heptane-2-carboxylic acid (BCH). Proline, glycine, cystine, basic (*e.g.* lysine and arginine) and acidic amino acids (e.g. glutamate and aspartate) did not inhibit [^{14}C]L-leucine uptake by S2-mock and S2-hLAT1 cells. [14] Consequently, the cell based data confirmed our previous results with rLAT1 expressing oocytes. The aim of the current work is to summarize our efforts and findings pertaining to the design and development of selective LAT1 inhibitors and to convey overall SAR findings.

Materials and Methods

(S)-2-Amino-3-phenylpropanoic acid (L-phenylalanine; **1**), (S)-2-amino-3-(3,4-dihydroxyphenyl)propanoic acid (L-Dopa; **2**), (S)-2-amino-3-(4-hydroxy-3-methoxyphenyl)propanoic acid (3-Methoxy-L-tyrosine monohydrate; **3**), (S)-2-amino-3-(4-(bis(2-chloroethyl)amino)phenyl)propanoic acid (melphalan; **4**), (2S)-2-amino-3-[4-(4-hydroxy-3-iodophenoxy)-3,5-diiodophenyl]propanoic acid (3,3',5 triiodothyronine, T3; **5**), (2S)-2-amino-3-[4-(4-hydroxy-3,5-diiodophenoxy)-3,5-diiodophenyl]propanoic acid (thyroxine, T4; **6**), methyl (2S)-2-amino-3-phenylpropanoate hydrochloride (L-Phenylalanine methyl ester hydrochloride; **7**), (2S)-2-(methylamino)-3-phenylpropanoic acid (N-Methyl-L-phenylalanine; **8**), 4-(2-aminoethyl)-1,2-benzenediol hydrochloride (Dopamine hydrochloride; **9**), 4-(2-aminoethyl)phenol (tyramine; **10**), (2S)-3-(3,4-dihydroxyphenyl)-2-hydrazino-2-methylpropanoic acid (carbidopa; **11**), (2S,3R)-2-amino-3-(3,4-dihydroxyphenyl)-3-hydroxypropanoic acid (droxidopa, L-DOPS; **12**), (R)-2-amino-3-phenylpropanoic acid (D-phenylalanine; **13**), (S)-2-amino-3-(4-hydroxyphenyl)propanoic acid (L-tyrosine; **14**), (S)-2-amino-3-(4-fluorophenyl)propanoic acid (L-4-fluorophenylalanine; **15**), (2S)-2-amino-2-methyl-3-phenylpropanoic acid (alpha-Methyl-L-phenylalanine; **16**), (2S)-2-amino-3-(4-hydroxyphenyl)-2-methylpropanoic acid (α-methyl-L-tyrosine; **17**), (R)-2-amino-3-hydroxy-2-(4-hydroxybenzyl)propanoic acid **18**, (S)-2-amino-3-hydroxy-2-(4-hydroxybenzyl)propanoic acid **19**, DL-3,5-difluorophenylalanine **20**; (S)-2-amino-3-(4-nitrophenyl)propanoic acid **21**; (S)-2-amino-3-(4-hydroxy-3-iodophenyl)propanoic acid (3-Iodo-L-Tyrosine; **23**), (S)-2-amino-3-(4-hydroxy-3,5-diiodophenyl)propanoic acid (3,5-diiodo-L-Tyrosine; **24**); (S)-2-amino-3,3-diphenylpropanoic acid **25**; 3-amino-3-(4-methoxy-phenyl)-propionic acid **26**; (S)-4-(2-amino-3-hydroxypropyl)phenol (L-Tyrosinol; **27)**, indoline-2-carboxylic acid **29**, 1,2,3,4-tetrahydro-3-isoquinoline-carboxylic acid HCl **30**; (S)-(-)-2-pyrrolidone-5-carboxylic acid (L-pyroglutamic acid; **31**), trans-4-hydroxy-L-proline **32**; (R)-2-hydroxy-2-phenylacetic acid ((R)-Mandelic Acid, **33**); (S)-2-hydroxy-2-phenylacetic acid ((S)-Mandelic Acid, **34**); 2-amino-3-(naphthalen-2-yl)propanoic acid (DL-3-(2-naphthyl)-alanine; **37**) (S)-2-amino-4-phenylbutanoic acid (L-homophenyl alanine HCl **38**), (S)-2-amino-3-(benzo[b]thiophen-3-yl)propanoic acid (3-(thianaphthen-3-yl)-L-alanine hydrochloride; **39**), triphenylphosphine (PPh_3), deuterated chloroform ($CDCl_3$), dimethyl sulfoxide (DMSO), ammonium acetate, formic acid, lithium hydroxide, bromine, chlorine, *N,N′*-diisopropylcarbodiimide (DIC), 2-(4-methoxyphenyl)ethanol, 2-(3-methoxyphenyl)ethanol, 2-(2-methoxyphenyl)ethanol, (2-methoxyphenyl)methanol, (3-(trifluoromethyl)phenyl)methanol, 2-(4-nitrophenyl)ethanol, (3-methoxyphenyl)methanol, (4-(trifluoromethyl)phenyl)methanol, (4-nitrophenyl)methanol, (4-methoxyphenyl)methanol, 2-(4-fluorophenyl)ethanol, 2-(3-fluorophenyl)ethanol,

2-(4-(trifluoromethyl)phenyl)ethanol, 2-(3-(trifluoromethyl)phenyl)ethanol, (2-fluorophenyl)methanol, 2-(2-(trifluoromethyl)phenyl)ethanol, (3-fluorophenyl)methanol, (4-fluorophenyl)methanol, 2-(4-(trifluoromethoxy)phenyl)ethanol, 2-phenylethanol, 2-(3,4-dimethoxyphenyl)ethanol, (3,4-dimethoxyphenyl)methanol, (2,3-dimethoxyphenyl)methanol, (2,3,4-trimethoxyphenyl)methanol, (4-methoxy-2,3-dimethylphenyl)methanol, (3,4,5-trimethoxyphenyl)methanol, (3,4,5-triethoxyphenyl)methanol, (3,4-diethoxyphenyl)methanol, benzo[d][1,3]dioxol-5-ylmethanol, pyridin-4-ylmethanol, (4-chlorophenyl)methanol, (2,3-difluorophenyl)methanol, (3,4,5-trifluorophenyl)methanol, (2,4-difluorophenyl)methanol, (4-chloro-2-methoxyphenyl)methanol. 2-(pyridin-2-yl)ethanol, pyridin-2-ylmethanol, pyridin-3-ylmethanol, (2-(trifluoromethyl)phenyl)methanol, (2,3,4,5,6-pentamethylphenyl)methanol, (3,5-bis(trifluoromethyl)phenyl)methanol, (perfluorophenyl)methanol, (4-(trifluoromethoxy)phenyl)methanol, (2,4-diethoxyphenyl)methanol, (4-methoxy-3-nitrophenyl)methanol, (2,6-dimethoxypyridin-3-yl)methanol were purchased from Sigma-Aldrich Chemical Company (St. Louis, MO). We monitored reactions via silica gel IB2-F thin layer chromatography (TLC) plates from J.T. Baker (Phillipsburg, NJ). Hexanes (Hex), HPLC grade methanol (MeOH), HPLC grade acetonitrile (ACN), HPLC grade water (H_2O) and ethyl acetate (EtOAc), and Tetrahydrofuran (THF) were from Fisher Scientific (Pittsburgh, PA). We purchased silica gel, standard grade, 60A, 4-63 μm from Sorbent Technologies (Norcross, GA). L-α-methyl-3-fluoro-tyrosine (FMT; **28**) was obtained from J-Pharma LTD.

NMR and LC/MS-MS

A 400 MHz Bruker NMR, Avance III 400 was used. An Applied Biosystems Sciex 4000 (Applied Biosystems; Foster City, CA) was used and included a Shimadzu HPLC (Shimadzu Scientific Instruments, Inc.; Columbia, MD) and Leap auto-sampler (LEAP Technologies; Carrboro, NC). Using a flow-rate of 0.4 mL/min, liquid chromatography employed an Agilent Technologies, Zorbax extended-C18 50 x 4.6 mm 5 micron column. It was equipped with a column guard at 40 ^{o}C. The mobile phase consisted of A: Water, 10 mM (NH_4OAc), 0.1% formic acid, and B: 1:1 methanol:acetonitrile. A total of 9.5 min run time, the chromatography method was 95% A held for 1.0 min; then ramped to 95% B at 3.0 min and held for 4.5 min, at which point it was brought back to 95% A at 8.5 min and held for 1.0 min. Synthesized compounds were monitored via electro-spray ionization positive ion mode (ESI+) using the following conditions: i) temperature, 450 ^{o}C; ii) curtain gas (CUR; set at 10) and Collisionally Activated Dissociation (CAD; set at 5) gas were nitrogen, iii) ion-spray voltage of 5500 V;; iv) quadruple one (Q1) and (Q3) were set on Unit resolution; v) dwell time was set at 200 msec, vi) Ion Source gas one (GS1) and two (GS2) were set at either 20 or 25,; vii) entrance potential set at 10 V; and viii) wcollision energy (CE), declustering potential (DP) and collision cell exit potential (CXP) are voltages (V). Samples (10 μL) were analyzed by LC/MS-MS. As judged by NMR and LC/MS-MS analysis, all purified compounds were > 97% pure.

Computational-based molecular modeling

Molecular modeling studies were conducted using Accelrys Discovery Studio 3.1 (Accelrys Software, Inc., San Diego, CA; http://accelrys.com). Crystallographic coordinates were downloaded from the protein data bank (http://www.pdb.org). The human LAT1 protein

homology model (residues 47-488) was constructed with the MODELLER protocol utilizing the crystal structure of the *Escherichia coli* AdiC amino acid antiporter as a template (PDB ID: 3L1L; ~40% similarity to the human LAT1 protein sequence). [15, 16] Structural coordinates of the bound Arg substrate from the AdiC crystal structure were transferred into the homology model during model construction to identify the amino acid binding site. No suitable templates for residues 1-46 and 489-507 of LAT1 were identified and therefore these residues were omitted from the model. The human LAT1 homology model was then subjected to energy minimization using the conjugate gradient minimization protocol (10,000 iterations) using a CHARMm forcefield and the Generalized Born implicit solvent model with simple switching. [17, 18] The flexible docking algorithm which allows for flexibility in both the ligand and receptor was used to predict the binding orientation of T3 **5**, T4 **6**, JPH203 **169** and its N-acetyl metabolite **175** within the binding site of the LAT1 homology model. [19] The protein-ligand complexes then underwent energy minimization *in situ* using the conjugate gradient method (10,000 iterations). The following residue side chains were designated as flexible for both the docking and minimization calculations: Ser66, Ile139, Ser143, Ser144, Phe252, Ser342, and Cys407. Binding energies were calculated for each of the resulting ligand poses without solvent correction and include the loss of conformational entropy and energy of the bound ligand. [20]

Synthesis: General Procedure

The corresponding di-protected (N-TFA-OMe) dihalo-tyrosine analog (2.22 mmol) was weighed into a dry round bottom flask (RBF; 100 mL) containing a stir-bar. The corresponding alcohol (2.34 mmol) and triphenylphosphine (4.46 mmol) were then added and diluted with anhydrous THF (25 mL), capped with a sure-seal and a N_2 balloon attached. The contents were stirred and cooled with an ice-bath (20 min) and then DIC (4.46 mmol) added dropwise via syringe transfer. The contents were then allowed to slowly warm to RT and stirred overnight and checked by TLC. The contents were concentrated under reduced pressure and silica gel added and subsequently purified by silica gel column chromatography; Hex → Hex:EtOAc (2:1). The isolated product was then transferred to a RBF (50 or 100 mL) containing a stir bar. THF (5 mL) was added and stirred into solution. The solution was cooled in an ice bath (20 min) and then 15 mL of ice cold 1.0 M LiOH was added. The contents were allowed to warm to ambient temperature and stirred over-night. The contents were again cooled into an ice bath (20 min) and THF removed under reduced pressure. Next, the pH was adjusted to pH ~3.0 with 3.0M HCl. The precipitant formed was collected via Büchner filtration and subsequently dried on the vacuum line overnight.

Results and Discussion

Using S2-hLAT1 and S2-hLAT2 cell lines, [^{14}C]L-leucine uptake inhibition was probed and average IC_{50} values reported. [14] We compared L-phenylalanine **1** versus D-phenylalanine **13** (**Table 1**; 11 μM versus 96 μM, respectively) which displays LAT1 was stereospecific in both species (rat and human). Compared to **1**, para-hydroxy analog **14** (L-tyrosine) displayed weaker competitive inhibition (essentially two fold) in both hLAT1 and hLAT2; as a phenol (pKa ~10), **14** has an intrinsic propensity to dissociate into the anion to produce a formal charge (-1) and negatively alter substrate interactions. Replacement of phenol **14** with fluoro **15** enhanced affinity and produced a more potent inhibitor, but it was not selective with LAT1 and LAT2 IC_{50} values essentially equal. Compared to **1** and **14**, α-methyl analogs (R_3 = methyl; **16** and **17**, respectively) produce weaker substrates/inhibitors. Therefore,

while LAT1 substrates and inhibitors may tolerate the α-methyl group, steric hindrance in this region becomes detrimental to substrate/inhibitor recognition. Illustrated by example **8** –NHMe, –NH_2 is an absolute chemical requirement. Regardless of stereochemistry, when R_3 becomes modified to –CH_2OH (**18** and **19**), it deters substrate/inhibitor interactions and we attribute these results to steric phenomena via -OH hydrogen bonding which distort an ideal zwitterion state (-NH_3^+/-CO_2^-). While not as potent as mono-fluoro analog **15**, difluoro **20** altered steric and electronics on the aromatic ring and produced LAT1:LAT2 selectivity; however, **20** was tested as the racemate. The change of -OH **14** to electron withdrawing nitro **21** produced a weaker LAT1 inhibitor; data further consistent with the notion that formal negative charge in this region becomes repulsive and decreases binding as previously discussed. Nitro analog **22** and iodo **23** further support the notion that electronics and steric factors in the aromatic region are critical to LAT1:LAT2 selectivity. The nitro analog has an intrinsic formal charge, while the bulky iodo does not. Interesting enough, the modification of mono-iodo **23** to di-iodo analog **24** began to produce compounds with moderate LAT1:LAT2 selectivity. Hindered **25** display the location where steric hindrance and subtle differences, relative to the amino acid, exist between LAT1 and LAT2. The amine location (**1** versus **26**) further supports the notion that tight charge distance between amine and carboxylic are required. Carboxylic acid **14** compared to alcohol **27** also support the amino acid zwitterion requirement. Comparing α-methyl **15** to α-methyl-fluoro **28** (FMT), both compounds display LAT1:LAT2 selectivity with the additional EWG decreasing LAT1 IC_{50} from 75 μM to 54 μM, respectively. Lastly, to further demonstrate the structural importance of the amino acid zwitterion state (-NH_3^+/-CO_2^-), we also tested compounds with modified –NH_2 such as indole **29**, isoquinoline **30**, L-pyroglutamic acid **31**, 4-hydroxy-L-proline **32**, and also replacement of –NH_2 with –OH, (R)-mandelic acid **33** and (S)-mandelic acid **34**; all of these compounds did not readily display LAT1 or LAT2 ^{14}C-Leu uptake inhibition.

Figure 1

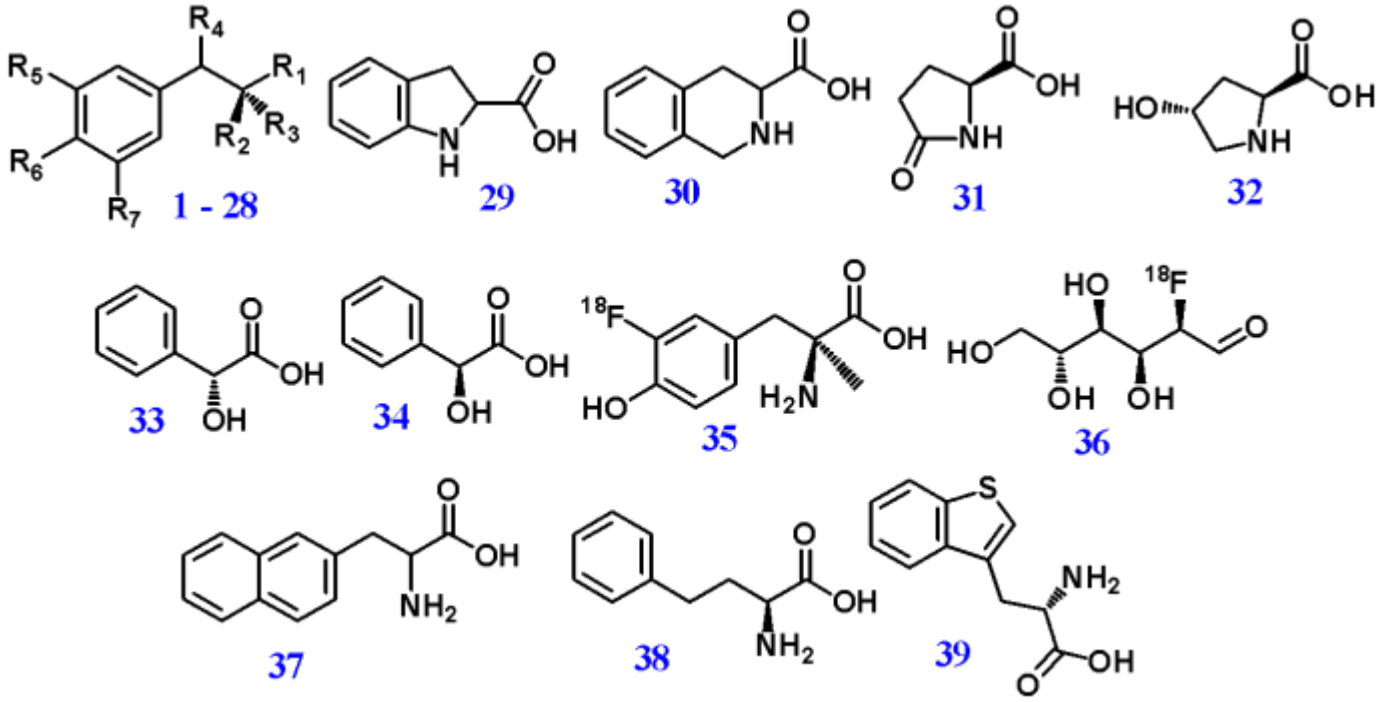

The experimental data summarized in **Table 1** demonstrate intrinsic chemical requirements to inhibit LAT1 amino acid substrates (*i.e.* ^{14}C-Leu). However, these data do not fully convey their potential as substrates. FMT is clinically important; the radiolabeled analog ^{18}F-FMT **29** has found use as a relatively new clinical diagnostic agent. Compared to fluoro-deoxyglucose [^{18}F]-FDG **30** for lung cancer primary tumor detection, [^{18}F]-FDG versus [^{18}F]-FMT exhibited sensitivity values of ~90% and ~94%, respectively. [11] As a functional imaging probe, [^{18}F]-FDG PET provides specificity and sensitivity in various cancer types. However, [^{18}F]-FDG is not specific for imaging malignant disease. As a result, [^{18}F]-FDG imaging data are known to produce false negative and false positive diagnoses. [21] Using hLAT1 and hLAT2 expressing oocytes and LC/MS-MS analysis, we sought to investigate uptake of **16** (MW = 195) and FMT **28** (MW = 215). Presented in **Figure 2**, are oocyte uptake experiments α-methyl-tyrosine **16** transport via LAT1 was faster than α-methyl-fluoro-tyrosine **28**; **16** and **28** displayed linear uptake at 5.0 μM (1.0 hr), while transport into the oocyte was saturable at 50.0 μM (K_m 27.1 ± 0.8 μM and 40.3 ± 0.8 μM, respectively). Compared to the LAT2 transport results – see supplementary materials section – both **16** and **28** displayed good LAT1 transport and inhibitory selectivity (**Table 1**). These features illustrate that a good PET probe such as 18F-FMT with an IC_{50} of LAT1 54 μM has room for improvement in the diagnostic area.

Figure 2

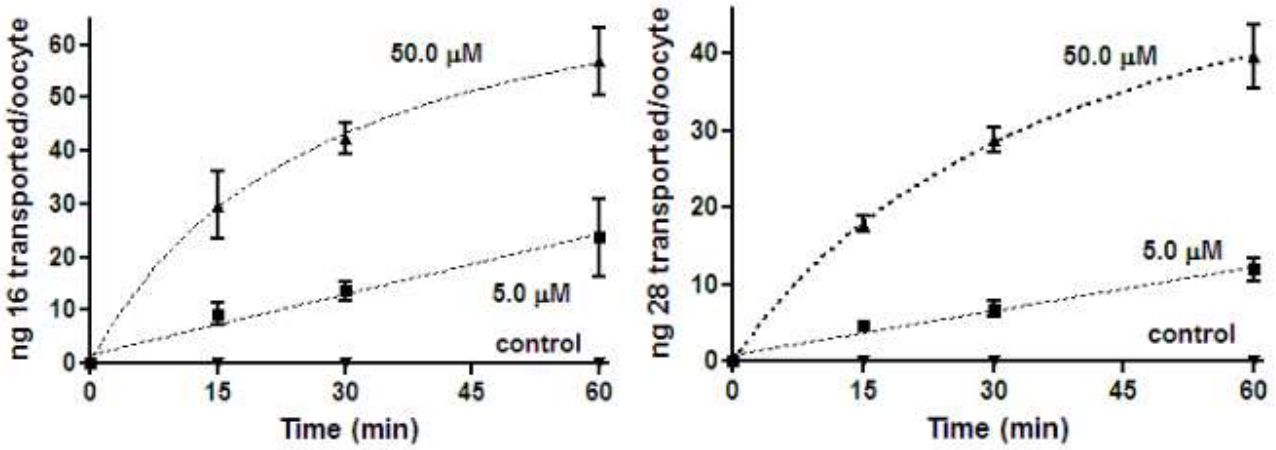

Since 2002, chemistry efforts in our laboratories have produced potent and LAT1 selective compounds. [22-23] The stereospecific zwitterion amino acid containing an aromatic ring (e.g. phenylalanine, tyrosine) comprises the LAT1 binding site (A-C; **Figure 3**). All experimental data suggest: i) amino acid functionality is required for binding (A) [13]; ii) amino acid L-stereochemistry is preferred and LAT1 may tolerate a methyl group at the alpha carbon (B); and iii) aromatic amino acids are preferred and size/electronic effects (C) clearly influence the substrate-inhibitor binding pocket interface. Iodo **23** and di-iodo **24** (**Table 1**) provided initial insight into how subtle differences in size and electronics ~5 ^{o}A away from the alpha carbon (**Figure 3**) may affect substrate/inhibitor properties. In addition to compounds in **Table 1**, we also tested DL-3-(2-naphthyl)-alanine **37**, L-homophenyl alanine **38**, and 3-(thianaphthen-3-yl)-L-alanine **39** (**Figure 1**) which afforded ^{14}C-Leu uptake S2-LAT1:S2-LAT2 IC_{50}'s (µM) of 30:112, 11:61 and 2.5:9.5, respectively. These data further confirmed that relative distance from the amino acid functionality and steric/electronic interactions are critical factors dictating LAT1:LAT2 selectivity. As we sought to fully understand the structural requirements to produce potent and selective LAT1 compounds, we systematically prepared and tested compounds containing the tyrosine chemical template.

Figure 3

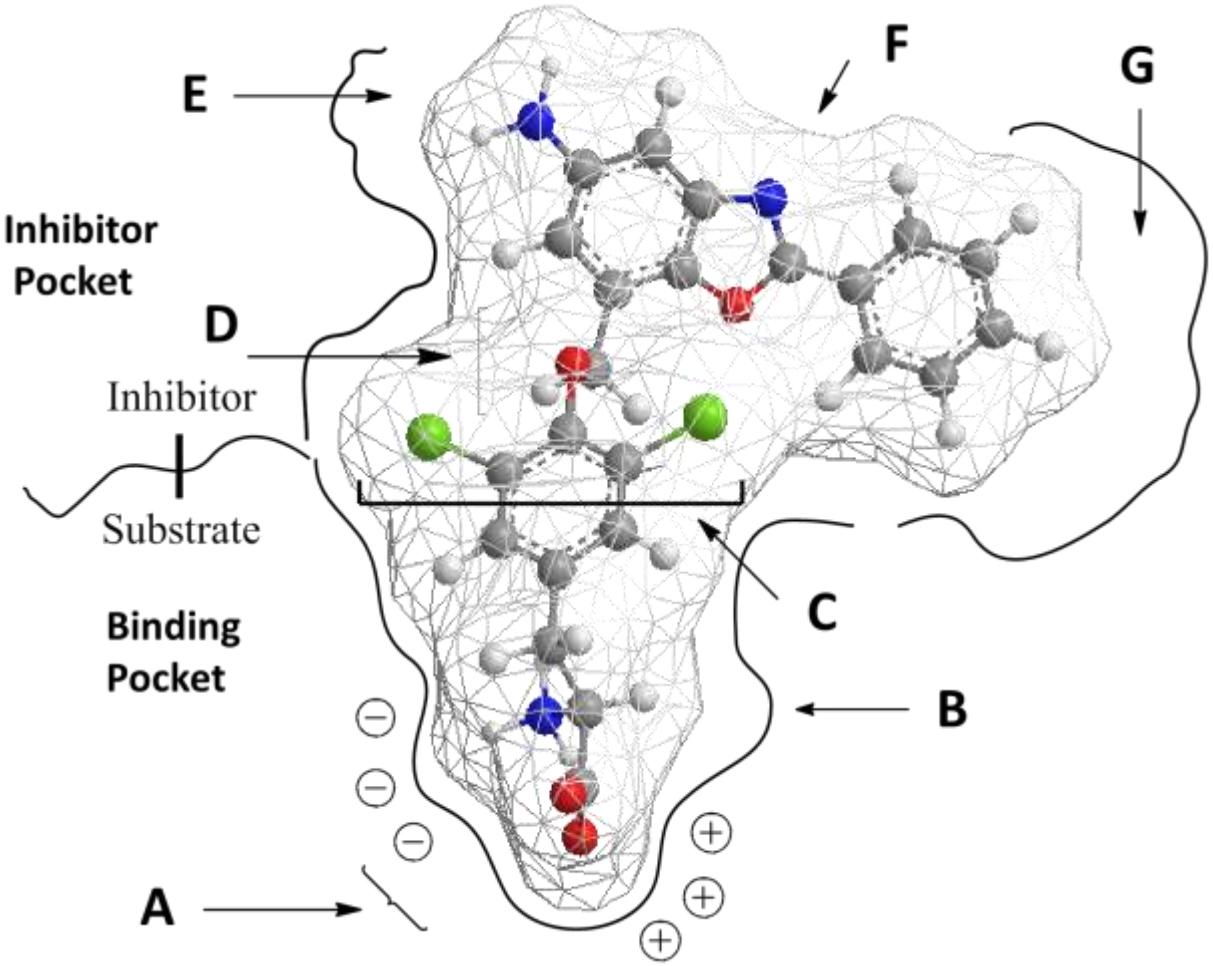

The general synthetic scheme to prepare compounds is presented in **Figure 4**. We prepared mono- and di-halogenated L-tyrosine compounds: monochloro **40**, dichloro **41**, dichloro-α-methyl **42**, and dibromo **43**. The amino acid functionality for these compounds and di-iodo **24** were di-protected by converting to their methyl esters followed by amine protection (-$COCF_3$) to give analogs **44 – 48**, respectively. Mono-iodo **23** and di-iodo **24** were previously discussed (**Table 1**); consistent with the iodo series, di-chloro **41** (37:NI μM; NI = no inhibition at 150 microM) was not as potent as mono-chloro **40** (19:12 μM) but displayed more profound LAT1:LAT2 selectivity. Hence, it is within this region where the first differences between LAT1 and LAT2 are experimentally observed; where amino acid analog molecular size begins to significantly influence selectivity and transport rates. We have termed this region as the "substrate-inhibitor interface" (**Figure 3**, C and D). Next, the di-protected di-halo-tyrosine compounds were chemically coupled with various alcohols and deprotected to produce a series of di-chloro (**49 - 96**; **Table 2**), di-bromo (**97 - 132**; **Table 3**) and di-iodo (**133 - 168**; **Table 4**) tyrosine compounds. These compounds were screened in the S2-hLAT1 and S2-hLAT2 cell system to afford the ^{14}C-Leu uptake inhibition data.

Figure 4

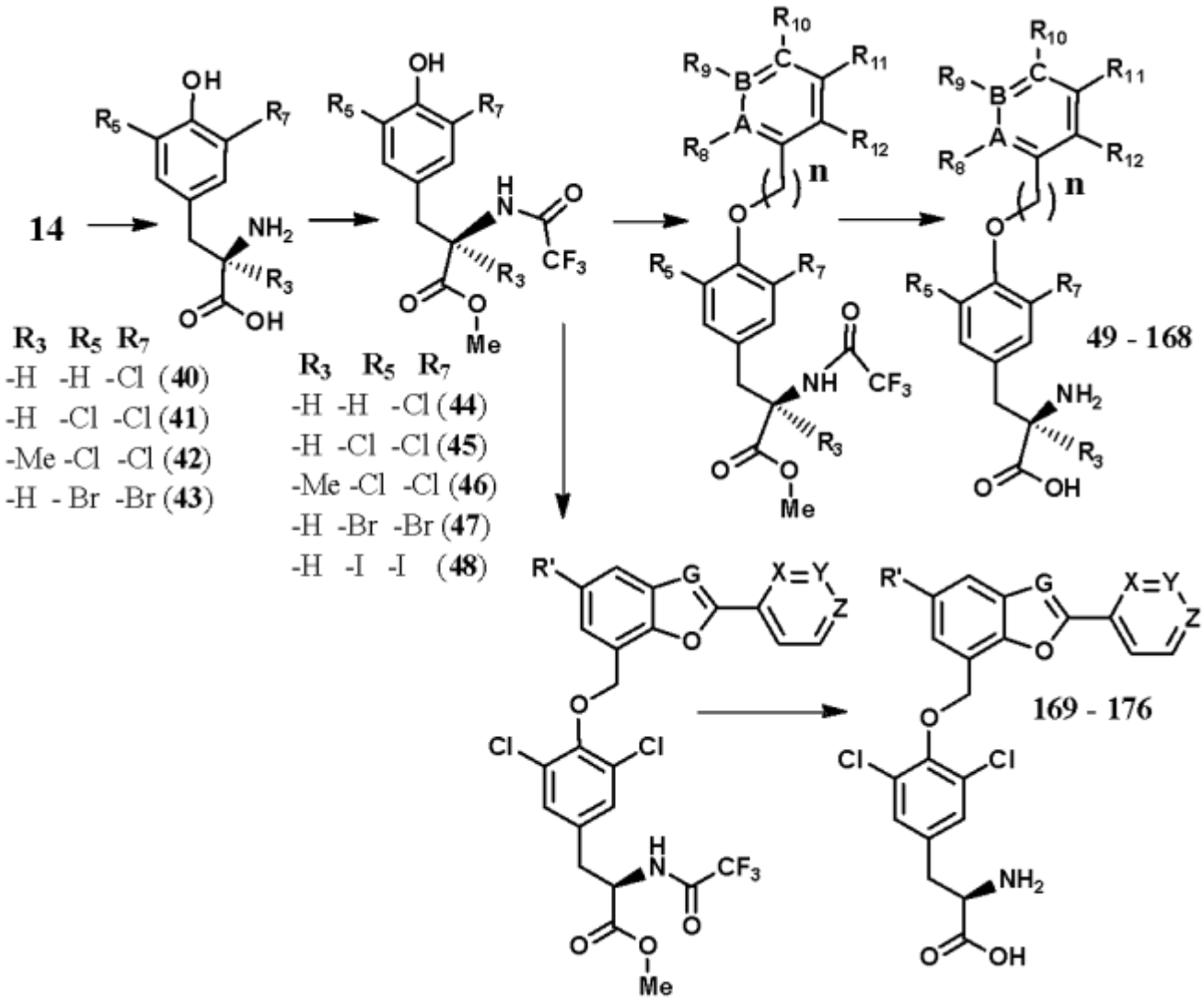

Table 2 Chlorinated Compounds - LAT1 and LAT2 ^{14}C-Leu Uptake Inhibition

#	R_3	R_5, R_7	n	R_8	R_9	R_{10}	R_{11}	R_{12}	A	B	C	LAT1	LAT2
49	H	di-Cl	1	O-Me	H	H	H	H	C	C	C	5.8	93.6
50	H	di-Cl	1	H	O-Me	H	H	H	C	C	C	13.6	28.3
51	H	di-Cl	1	H	H	O-Me	H	H	C	C	C	16.8	59.7
52	H	di-Cl	1	O-Me	O-Me	H	H	H	C	C	C	28.2	NI
53	H	di-Cl	1	H	O-Me	O-Me	H	H	C	C	C	17.8	NI
54	H	di-Cl	1	O-Me	H	O-Me	H	H	C	C	C	0.8	5.5
55	H	di-Cl	1	O-Me	O-Me	O-Me	H	H	C	C	C	8.1	NI
56	H	di-Cl	1	Me	Me	O-Me	H	H	C	C	C	3.5	NI
57	H	di-Cl	1	H	O-Me	O-Me	O-Me	H	C	C	C	9.4	NI
58	H	di-Cl	1	O-Me	H	O-Me	O-Me	H	C	C	C	29.2	NI
59	H	di-Cl	1	O-Me	LP	O-Me	H	H	C	N	C	2.4	32.5
60	H	di-Cl	1	O-Me	H	Cl	H	H	C	C	C	4.4	NI
61	H	di-Cl	1	H	H	NO_2	H	H	C	C	C	62.4	23.1
62	H	di-Cl	1	H	NO_2	O-Me	H	H	C	C	C	8.4	126
63	H	di-Cl	1	H	O-Et	O-Et	H	H	C	C	C	2.9	44.9
64	H	di-Cl	1	H	O-Et	O-Et	O-Et	H	C	C	C	1.2	NI
65	H	di-Cl	1	O-Et	H	O-Et	H	H	C	C	C	2.2	NI
66	H	di-Cl	1	LP	H	H	H	H	N	C	C	93.3	NI
67	H	di-Cl	1	H	LP	H	H	H	C	N	C	106	NI
68	H	di-Cl	1	H	H	LP	H	H	C	C	N	NI	NI
69	H	di-Cl	1	H	H	F	H	H	C	C	C	10.2	19.0
70	H	di-Cl	1	H	F	F	H	H	C	C	C	NI	NI
71	H	di-Cl	1	CF_3	H	H	H	H	C	C	C	19.4	NI
72	H	di-Cl	1	H	CF_3	H	H	H	C	C	C	22.3	86.3
73	H	di-Cl	1	H	H	CF_3	H	H	C	C	C	10.1	14.4
74	H	di-Cl	1	H	O-CH2-	O	H	H	C	C	C	4.2	27.3
75	H	di-Cl	2	H	H	H	H	H	C	C	C	50.7	NI
76	H	di-Cl	2	H	H	O-Me	H	H	C	C	C	25.3	NI
77	H	di-Cl	2	H	O-Me	H	H	H	C	C	C	4.2	86.7
78	H	di-Cl	2	O-Me	H	H	H	H	C	C	C	3.4	NI
79	H	di-Cl	2	H	H	CF_3	H	H	C	C	C	1.3	NI
80	H	di-Cl	2	H	CF_3	H	H	H	C	C	C	13.2	NI
81	H	di-Cl	2	CF_3	H	H	H	H	C	C	C	NI	NI
82	H	di-Cl	2	H	H	F	H	H	C	C	C	34.5	NI
83	H	di-Cl	2	H	F	H	H	H	C	C	C	37.4	61.3
84	H	di-Cl	2	F	H	H	H	H	C	C	C	35.1	56.0
85	H	di-Cl	2	H	H	NO_2	H	H	C	C	C	19.8	NI
86	H	di-Cl	2	H	H	O-CF_3	H	H	C	C	C	7.7	NI
87	H	H, Cl	2	O-Me	H	O-Me	H	H	C	C	C	NI	NI
88	H	H, Cl	2	H	H	O-Me	H	H	C	C	C	NI	NI
89	Me	di-Cl	1	H	H	CF_3	H	H	C	C	C	99.9	NI
90	Me	di-Cl	1	H	H	O-Me	H	H	C	C	C	6.7	16.4
91	Me	di-Cl	1	H	O-Me	H	H	H	C	C	C	NI	NI

92	Me	di-Cl	1	O-Me	H	H	H	H	C	C	C	NI	NI
93	Me	di-Cl	1	O-Me	O-Me	H	H	H	C	C	C	NI	NI
94	Me	di-Cl	1	H	O-Me	O-Me	H	H	C	C	C	NI	NI
95	Me	di-Cl	1	H	O-Me	O-Me	O-Me	H	C	C	C	NI	NI
96	Me	di-Cl	1	H	H	LP	H	H	C	C	N	NI	NI

NI = no inhibition at 150 microM

Figure 5

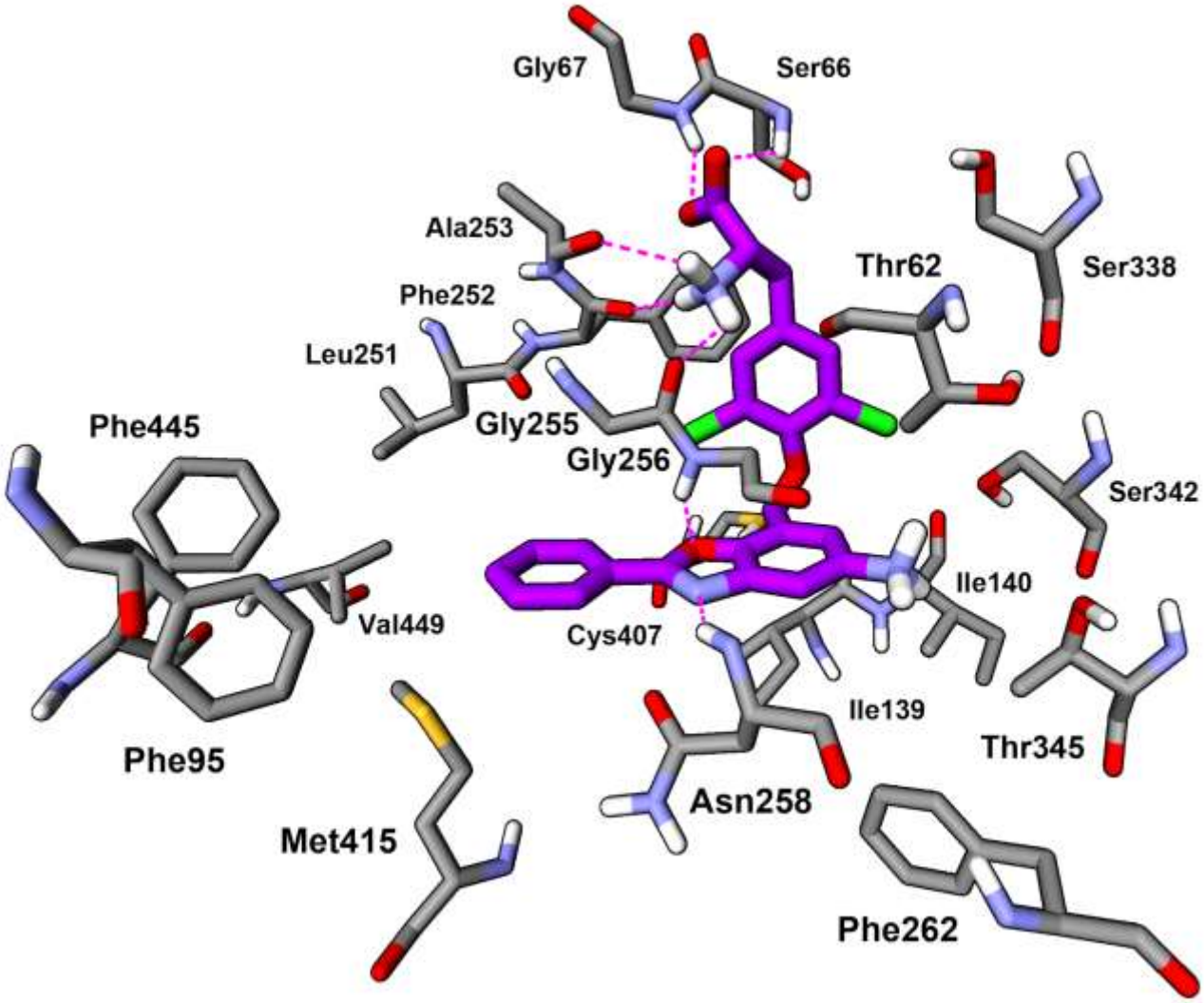

Table 3 Brominated Compounds - LAT1 and LAT2 ^{14}C-Leu Uptake Inhibition

#	R_3	R_5, R_7	n	R_8	R_9	R_{10}	R_{11}	R_{12}	A	B	C	LAT1	LAT2
97	H	di-Br	1	O-Me	H	H	H	H	C	C	C	10.2	NI
98	H	di-Br	1	H	O-Me	H	H	H	C	C	C	67.1	NI
99	H	di-Br	1	H	H	O-Me	H	H	C	C	C	16.4	86.5
100	H	di-Br	1	H	CF_3	H	H	H	C	C	C	NI	NI
101	H	di-Br	1	H	H	CF_3	H	H	C	C	C	NI	NI
102	H	di-Br	1	H	H	NO_2	H	H	C	C	C	29.2	5.5
103	H	di-Br	1	F	H	H	H	H	C	C	C	NI	69.1
104	H	di-Br	1	H	F	H	H	H	C	C	C	71.5	49.3
105	H	di-Br	1	H	H	F	H	H	C	C	C	33.4	42.5
106	H	di-Br	1	H	O-Me	O-Me	H	H	C	C	C	23.3	130
107	H	di-Br	1	O-Me	O-Me	H	H	H	C	C	C	27.5	NI
108	H	di-Br	1	O-Me	O-Me	O-Me	H	H	C	C	C	12.1	NI
109	H	di-Br	1	Me	Me	O-Me	H	H	C	C	C	18.1	NI
110	H	di-Br	1	H	O-Me	O-Me	O-Me	H	C	C	C	9.4	NI
111	H	di-Br	1	H	O-Et	O-Et	O-Et	H	C	C	C	2.1	NI
112	H	di-Br	1	H	O-Et	O-Et	H	H	C	C	C	2.6	35.7
113	H	di-Br	1	H	O-CH2-	O	H	H	C	C	C	22.0	NI
114	H	di-Br	1	H	H	LP	H	H	C	C	N	NI	NI
115	H	di-Br	1	H	H	Cl	H	H	C	C	C	15.5	40.3
116	H	di-Br	1	F	F	H	H	H	C	C	C	88.0	42.2
117	H	di-Br	1	H	F	F	F	H	C	C	C	59.5	NI
118	H	di-Br	1	F	H	F	H	H	C	C	C	38.5	43.8
119	H	di-Br	1	O-Me	H	Cl	H	H	C	C	C	6.7	NI
121	H	di-Br	2	H	O-Me	H	H	H	C	C	C	6.3	NI
122	H	di-Br	2	O-Me	H	H	H	H	C	C	C	5.4	NI
123	H	di-Br	2	H	H	CF_3	H	H	C	C	C	43.2	NI
124	H	di-Br	2	H	CF_3	H	H	H	C	C	C	31.8	NI
125	H	di-Br	2	CF_3	H	H	H	H	C	C	C	NI	NI
126	H	di-Br	2	H	H	NO_2	H	H	C	C	C	19.5	NI
127	H	di-Br	2	H	H	F	H	H	C	C	C	42.3	NI
128	H	di-Br	2	H	F	H	H	H	C	C	C	22.2	NI
129	H	di-Br	2	F	H	H	H	H	C	C	C	37.1	91.9
130	H	di-Br	2	H	H	H	H	H	C	C	C	19.9	NI
131	H	di-Br	2	H	O-Me	O-Me	H	H	C	C	C	3.9	NI
132	H	di-Br	2	H	H	O-CF_3	H	H	C	C	C	8.3	NI

NI = no inhibition at 150 microM

Table 4 Iodo Compounds - LAT1 and LAT2 ^{14}C-Leu Uptake Inhibition

#	R_3	R_5, R_7	n	R_8	R_9	R_{10}	R_{11}	R_{12}	A	B	C	LAT1	LAT2
133	H	di-I	1	H	H	Cl	H	H	C	C	C	10.4	29.5
134	H	di-I	1	LP	H	H	H	H	N	C	C	8.0	NI
135	H	di-I	1	H	LP	H	H	H	C	N	C	86.0	NI
136	H	di-I	1	H	H	LP	H	H	C	C	N	57.0	NI
137	H	di-I	1	O-Me	H	H	H	H	C	C	C	17.8	NI
138	H	di-I	1	H	O-Me	H	H	H	C	C	C	NI	NI
139	H	di-I	1	H	H	O-Me	H	H	C	C	C	18.6	NI
140	H	di-I	1	H	O-Me	O-Me	H	H	C	C	C	19.2	95.6
141	H	di-I	1	H	H	CF_3	H	H	C	C	C	84.7	7.7
142	H	di-I	1	CH_3	CH_3	CH_3	CH_3	CH_3	C	C	C	NI	NI
143	H	di-I	1	H	CF_3	H	CF_3	H	C	C	C	NI	NI
144	H	di-I	1	F	H	H	H	H	C	C	C	29.8	7.4
145	H	di-I	1	H	F	H	H	H	C	C	C	42.5	12.9
146	H	di-I	1	H	H	F	H	H	C	C	C	10.0	11.1
147	H	di-I	1	F	F	H	H	H	C	C	C	27.0	13.9
148	H	di-I	1	F	H	F	H	H	C	C	C	14.0	5.5
149	H	di-I	1	H	F	F	F	H	C	C	C	17.3	30.6
150	H	di-I	1	F	F	F	F	F	C	C	C	48.3	NI
151	H	di-I	1	O-Me	O-Me	O-Me	H	H	C	C	C	23.6	NI
152	H	di-I	1	Me	Me	O-Me	H	H	C	C	C	7.7	NI
153	H	di-I	1	H	O-Me	O-Me	O-Me	H	C	C	C	15.0	NI
154	H	di-I	1	H	O-Et	O-Et	O-Et	H	C	C	C	6.2	NI
155	H	di-I	1	O-Et	H	O-Et	H	H	C	C	C	17.2	NI
157	H	di-I	1	H	O-CH_2-	O	H	H	C	C	C	24.1	NI
158	H	di-I	2	LP	H	H	H	H	N	C	C	27.3	NI
159	H	di-I	2	H	O-Me	H	H	H	C	C	C	7.1	NI
160	H	di-I	2	O-Me	H	H	H	H	C	C	C	3.9	NI
161	H	di-I	2	H	O-Me	O-Me	H	H	C	C	C	4.8	NI
162	H	di-I	2	H	H	CF_3	H	H	C	C	C	7.4	NI
163	H	di-I	2	H	CF_3	H	H	H	C	C	C	NI	NI
164	H	di-I	2	CF_3	H	H	H	H	C	C	C	NI	NI
165	H	di-I	2	H	H	F	H	H	C	C	C	NI	NI
166	H	di-I	2	H	F	H	H	H	C	C	C	67.0	NI
167	H	di-I	2	F	H	H	H	H	C	C	C	54.5	NI
168	H	di-I	2	H	H	O-CF_3	H	H	C	C	C	NI	NI

NI = no inhibition at 150 microM

The data summarized in **Tables 2-4** produced general trends: i) overall, di-chloro-analogs exert a better fit within the LAT1 binding/substrate pocket than their corresponding di-bromo and di-iodo analogs (*e.g.* compare **49**, **97** to **137**; and also compare **64, 111** to **154**); and ii) that electronic and/or hydrogen bonding interactions far from the amino acid may significantly influence inhibitor potency. To help illustrate this major finding, we have summarized a series of potent LAT1 inhibitors (**Figure 4** & **Table 5**) which maintain the dichloro-tyrosine functionality but modified with aro-substituted benzo[d]oxazol-5-amines (**169 – 176**). Compound **169** (JPH203) has a low nano-molar *in vitro* inhibitory activity and the importance of the aryl amine may be exemplified by comparing **169** to dimethyl analogs **170 - 174** resulting in altered IC_{50} LAT1 values. [24] Region E (**Figure 3**) contains limited space but may accommodate minor modifications such as –NHCOMe, –NHMe, -NMe_2, -F, -CF_3; the metabolite of JPH203 **169**, NAc-JPH203 **175** , was an active metabolite albeit a weaker LAT1 inhibitor. [25] Comparing **170** to benzofuran **171** demonstrates the importance of the nitrogen atom in region F (**Figure 3**). Modifying phenylbenzo[d]oxazol-5-amine **170** with a nitrogen atom in the para-, meta- or ortho- position (**172, 173** and **174**, respectively; **Table 5**) produced weaker LAT1 inhibitors. Amine **176**, compared to **173** (**Table 5**), further illustrates that –NH_2 is preferred (region E, **Figure 3**) and that slight secondary pocket modification may have profound changes in inhibitory potency. The phenyl ring, region G, should not be electronically distorted with a hydrogen-bonding group (*e.g.* pyridinyl or phenol) as they significantly alter both inhibitor potency and/or LAT1:LAT2 selectivity. We know from examples **169** versus **177** (**Table 5**) that hydrogen bonding and the ability to form a formal charge in the inhibitory pocket severely alters LAT1:LAT2 selectivity (consistent with observations previously discussed, **Tables 1 – 4**).

Table 5 JPH203 and derivatives

Compound	R'	G	X	Y	Z	LAT1 (nM)	LAT2 (μM)
169 (JPH203)	NH_2	N	CH	CH	CH	42	> 100
170	NMe_2	N	CH	CH	CH	91	> 100
171	NMe_2	CH	CH	CH	CH	3880	> 100
172	NMe_2	N	CH	CH	N	589	> 100
173	NMe_2	N	CH	N	CH	2008	> 100
174	NMe_2	N	N	CH	CH	1307	> 100
175 (NAc-JPH203)	$NHCOCH_3$	N	CH	CH	CH	240	> 100
176	NH_2	N	CH	N	CH	168	> 100
177	H	N	CH	CH	OH	120	200 nM

JPH203 is currently in Phase II clinical trials in Japan. The first Phase I trial of JPH203 was conducted in Japan and designed to determine maximum tolerated dose and safety. Seventeen patients were enrolled in the Phase I and were intravenously administered JPH203 for seven days

with doses ranging from 12-110 mg/m^2. Using a 3 + 3 design, dose limiting toxicity was evaluated in the first cycle. The data was consistent with a maximum tolerated dose of 60 mg/m^2. The recommended Phase II dose was 25 mg/m^2. Overall, JPH203 was well tolerated and had promising results in biliary tract cancer.

Regarding computational analysis, the binding orientation of Arg transferred into the homology model from the crystal structure template indicates that the predicted binding site for the amino acid moiety is comprised of Ser66, Gly67, Phe252, Ala253, and Gly255, while the basic side chain occupies a binding pocket consisting of Ile139, Ile140, Ser342, Thr345, and Cys407 (JPH203, **Figure 5**). *In silico* small molecule docking of T3, T4, JPH203 and NAc-JPH203 indicates the amino acid moiety of the compound to bind in a manner similar to Arg, (**Supplementary Figure 3**) with the amine substituent occupying the binding site of the basic side chain and the phenyl ring occupying an adjacent hydrophobic pocket consisting of Phe95, Met415, Phe445, and Val449. Although the amino acid moiety of the NAc JPH203 (**Supplementary Figure 4**) metabolite is predicted to bind the amino acid binding site, the region where the primary amine of the parent compound is predicted to bind does not appear to have the capacity to accommodate the *N*-acetyl group. Therefore the binding orientation of the NAc derivative is predicted to be flipped across the ester bond compared to the parent compound, with the NAc group predicted to occupy the hydrophobic pocket (**Supplementary Figure 4**). This resulted in a substantially less favorable predicted binding energy for metabolite NAc-JPH203 (-73.9 kcal/mol vs -163.7 kcal/mol). This is consistent with our *in vitro* LAT1 activity data indicating a rough 5-fold higher IC_{50} for the metabolite compared to JPH203. [25] The *in vitro* LAT1 inhibitory trend for these compounds was **169** > **175** > **5** > **6** and consistent with an *in silico* binding energy trend (kcal/mol) of -198.8 > -138.5 > -132.4 > -65.2, respectively.

To our knowledge, this is the first report providing a summary regarding LAT1 substrate/inhibitor interface and how subtle differences in the various regions within LAT1 versus LAT2 exist. Herein, we provide historical aspects regarding initial Structure Activity Relationship (SAR) findings reported in 2002 with the oocyte model and in 2008 with S2-LAT1 and S2-LAT2 cell lines. We summarize a series of dichloro- dibromo- and diiodo- tyrosine analogs, and tested their potential to inhibit leucine transport in vitro to afford IC_{50} values with a few being low microM LAT1 inhibitors. We then summarize our efforts regarding novel LAT1 inhibitors with sub-nanomolar (nM) IC_{50}'s to produce JPH203. We describe differences observed between LAT1 and LAT2. Overall, we provide an expanded SAR model regarding potent and selective LAT1 inhibitors.

Acknowledgements:

Research was funded by J-Pharma Co., Ltd. (Tokyo, Japan.) and Translational Research Promotion Project, NEDO, METI in Japan, and also utilized services of the Medicinal Chemistry Core facility (MCC; MFW) housed within the Department of Pharmaceutical Sciences (DOPS) in the Skaggs School of Pharmacy and Pharmaceutical Sciences.

Supplementary materials

Supplementary Figure 1

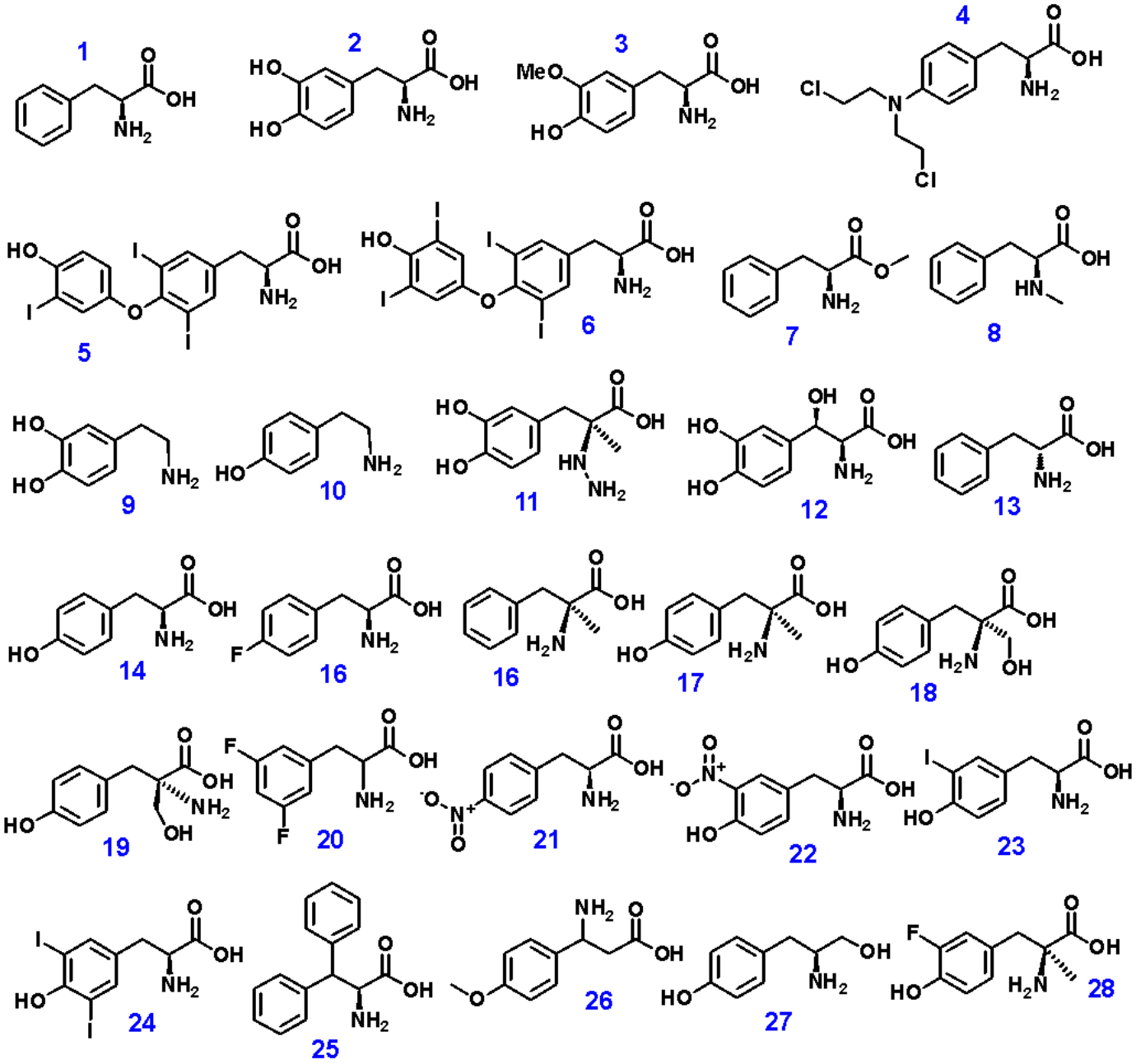

Supplementary Figure 2

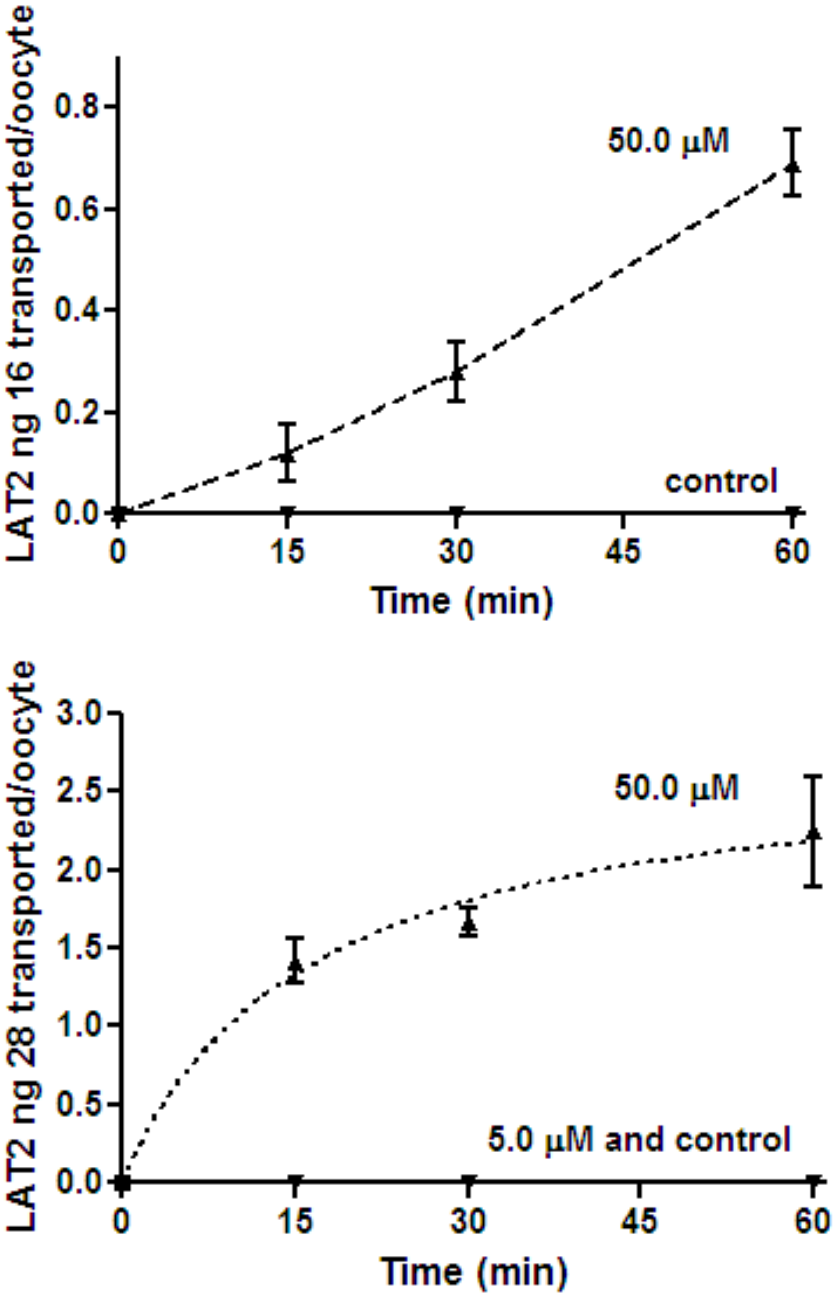

Supplementary Figure 3

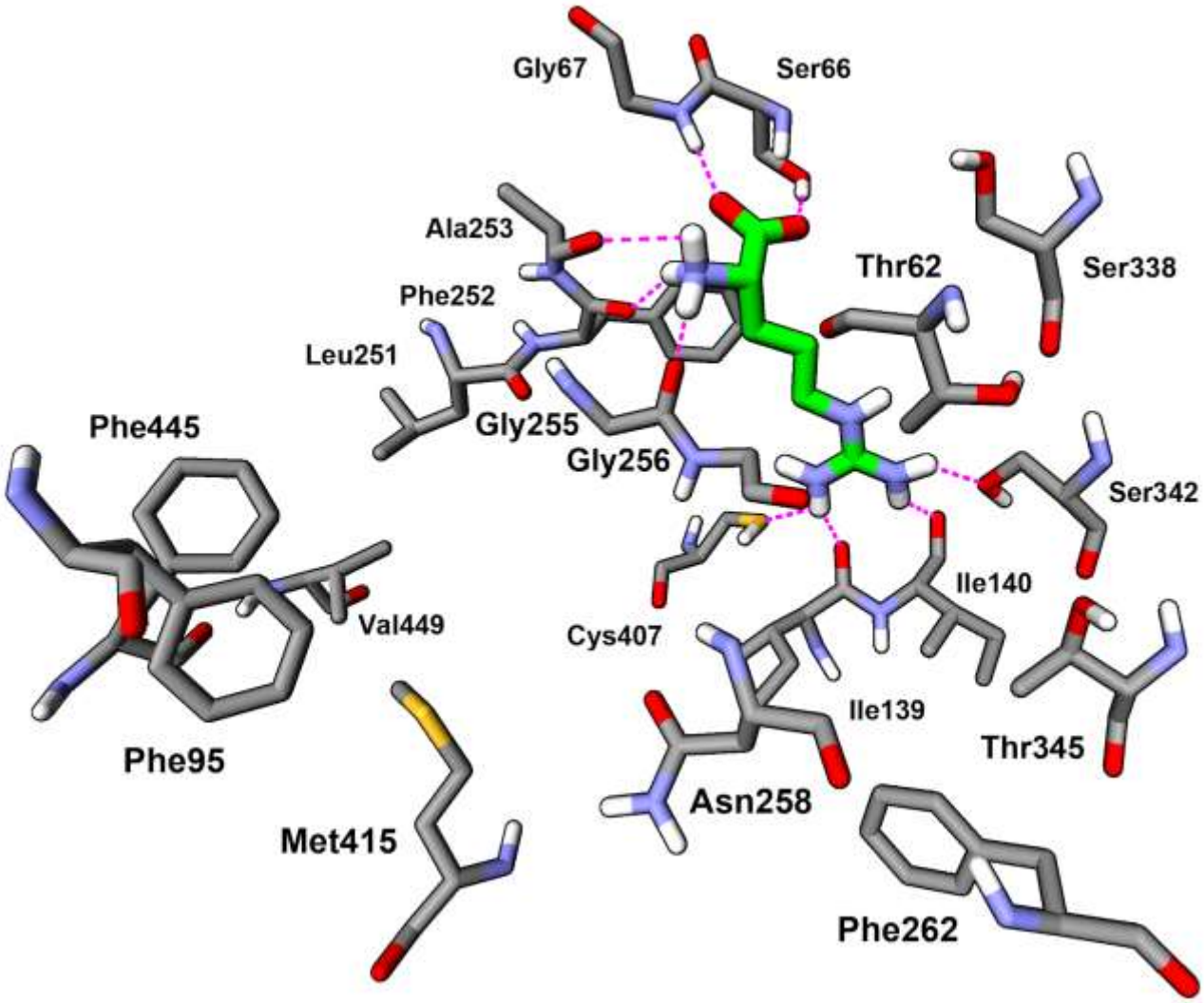

Supplementary Figure 4

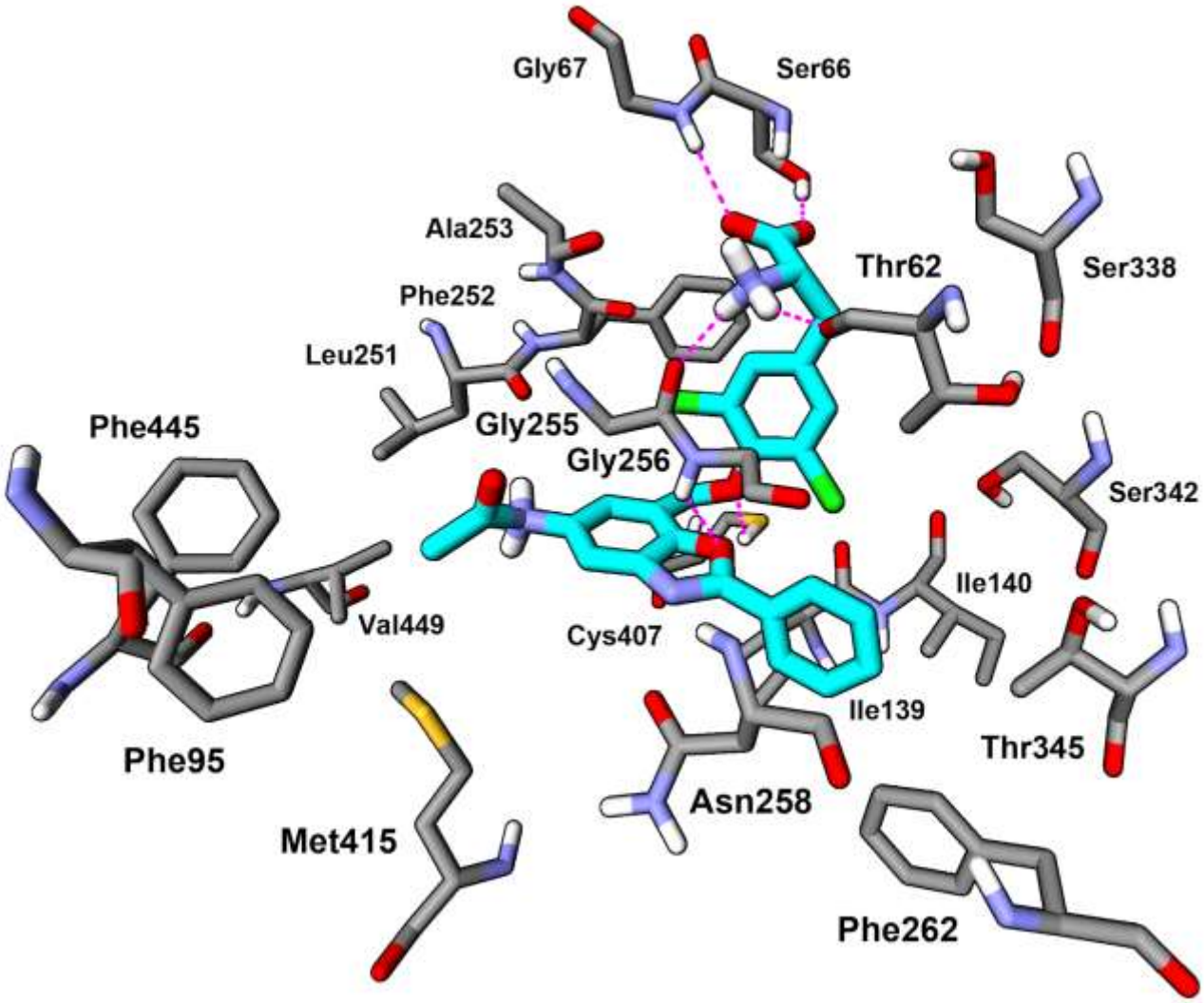

References

1. Kanai, Y., Segawa, H., Miyamoto, K., Uchino, H., Takeda, E., Endou, H., 1998. Expression cloning and characterization of a transporter for large neutral amino acids activated by the heavy chain of 4F2 antigen (CD98). J. Biol. Chem. 273, 23629-23632.
2. Segawa, H., Fukasawa, Y., Miyamoto, K., Takeda, E., Endou, H., Kanai, Y., 1999. Identification and functional characterization of a Na^+-independent neutral amino acid transporter with broad substrate selectivity. J. Biol. Chem. 274, 19745-19751.
3. Babu, E., Kanai, Y., Chairoungdua, A., Kim, D.K., Iribe, Y., Tangtrongsup, S., Jutabha, P., Li, Y., Ahmend, N., Sakamoto, S., Anzai, N., Nagamori, S., Endou, H., 2003. Identification of a novel system L amino acid transporter structurally distinct from heterodimeric amino acid transporters. J. Biol. Chem. 278, 43838-43845.
4. Bodoy, S., Martin, L., Zorzano, A., Palacin, M., Estevez, R., Bertran, J., 2005. Identification of LAT4, a novel amino acid transporter with system L activity. J. Biol. Chem. 280, 12002-12011.
5. Fukasawa, Y., Segawa, H., Kim, J.Y,, Charoungdua, A., Kim, D.K., Endou, H., Endou, Y., 2000. Identification and characterization of a Na+-independent neutral amino acid transporter which associates with the 4F2 heavy chain and exhibits selectivity for small neutral D- and L-amino acids. J. Biol. Chem. 275, 9690-9698.
6. Yanagida, O., Kanai, Y., Chairoungdua, A., Kim, D.K., Segawa, H., Nii, T., Cha, S.H., Matsuo, H., Fukushima, J., Fukasawa, Y., Tani, Y., Taketani, Y., Uchino, H., Kim, J.Y., Inatomi, J., Okayasu, I., Miyamoto, K., Takeda, E., Goya, T., Endou, H., 2001. Human L-type amino acid transporter 1 (LAT1): characterization of function and expression in tumor cell lines. Biochim. Biophys. Acta. 1514, 291-302.
7. Ohkame, H., Masuda, H., Ishii, Y., Kanai, Y., 2001. Expression of L-type amino acid transporter 1 (LAT1) and 4F2 heavy chain (4F2hc) in liver tumor lesions of rat models. J. Surg. Oncol. 78, 265-271.
8. Kobayashi, H., Ishii, Y., Takayama, T., 2005. Expression of L-type amino acid transporter 1 (LAT1) in esophageal carcinoma. J. Surg. Oncol. 90, 233-238.
9. Nakanishi, K., Matsuo, H., Kanai, Y., Endou, H., Hiroi, S., Tominaga, S., Mukai, M., Ikeda, E., Ozeki, Y., Aida, S., Kawai, T., 2006. LAT1 expression in normal lung and in atypical adenomatous hyperplasia and adenocarcinoma of the lung. Virchows Arch. 448, 142-150.
10. Nawashiro, H., Otani, N., Shinomiya, N., Fukui, S., Ooigawa, H., Shima, K., Matsuo, H., Kanai, Y., Endou, H., 2006. L-type amino acid transporter 1 as a potential molecular target in human astrocytic tumors. Int. J. Cancer. 119, 484-492.
11. Kaira, K., Oriuchi, N., Otani, Y., Shimizu, K., Tanaka, S., Imai, H., Yanagitani, N., Sunaga, N., Hisada, T., Ishizuka, T., Dobashi, K., Kanai, Y., Endou, H., Nakajima, T., Endo, K., Mori, M., 2007. Fluorine-18-alpha-methyltyrosine positron emission tomography for diagnosis and staging of lung cancer: a clinicopathologic study. 13, 6369-6378.
12. Sakata, T., Ferdous, G., Tsuruta, T., Satoh, T., Baba, S., Muto, T., Ueno, A., Kanai, Y., Endou, H., Okayasu, T., 2009. L-type

amino-acid transporter 1 as a novel biomarker for high-grade malignancy in prostate cancer. Path. Int. 59, 7-18.

13. Uchino, H., Kanai, Y., Kim, D.K., Wempe, M.F., Chairoungdua, A., Morimoto, E., Anders, M.W., Endou, H., 2002. Transport of amino acid-related compounds mediated by L-type amino acid transporter 1 (LAT1): insights into the mechanisms of substrate recognition. Mol. Pharmacol. 61, 729-737.
14. Morimoto, E., Kanai, Y., Kim, do. K., Chairoungdua, A., Choi, H.W., Wempe, M.F., Anzai, N., Endou, H., 2008. Establishment and characterization of mammalian cell lines stably expressing human L-type amino acid transporters. J. Pharmacol. Sci. 108, 505-516.
15. Eswar N, Eramian D, Webb B, Shen MY, Sali A. Protein structure modeling with MODELLER. Methods Mol Biol. 2008; 426:145-59.
16. Gao X, Zhou L, Jiao X, Lu F, Yan C, Zeng X, Wang J, Shi Y. Mechanism of substrate recognition and transport by an amino acid antiporter. Nature 2010 463(7282):828-32.
17. Fletcher, R, Reeves, CM. Function Minimization by Conjugate Gradients. Comput. J. 1964, 7, 149-154.
18. Feig M, Onufriev A, Lee MS, Im W, Case DA, Brooks CL. Performance comparison of generalized born and Poisson methods in the calculation of electrostatic solvation energies for protein structures. J Comput Chem 2004; 25:265-284.
19. Koska J, Spassov VZ, Maynard AJ, Yan L, Austin N, Flook PK and Venkatachalam CM. Fully automated molecular mechanics based induced fit protein-ligand docking method. J Chem Inf Model 2008, 48(10): 1965-1973.
20. Tirado-Rives J and Jorgensen WL. Contribution of conformer focusing to the uncertainty in predicting free energies for protein-ligand binding. J Med Chem 2006, 49, 5880-5884.
21. Vallabhajosula, S., 2007. ^{18}F-labeled positron emission tomographic radiopharmaceuticals in oncology: an overview of radiochemistry and mechanisms of tumor localization. Semin. Nucl. Med. 37, 400-419.
22. Endou, H., Kanai, Y., Tsujihara, K., Saito, K., 2008. Aromatic Amino Acid Derivatives and Medicinal Compositions. US Patent 7,345,068 B2.
23. Wempe, M.F., Endou, H. 2011. Alpha-substituted and alpha-unsubstituted aromatic amino acid derivatives and compositions thereof for use to treat, diagnose, or monitor a medical considition. US Patent Application 20110150767.
24. Oda, K., Hosoda, N., Endo, H., Saito, K., Tsujihara, K., Yamamura, M., Sakata, T., Anzai, N., Wempe, M.F., Kanai, Y., Endou, H., 2010. L-type Amino Acid Transporter 1 Inhibitors Inhibit Tumor Cell Growth. Cancer Science, 101, 173-179.
25. Wempe, M.F., Rice, P.J., Lightner, J.W., Jutabha, P., Hayashi, M., Anzai, N., Wakui, S., Kusuhara H., Sugiyama, Y., Endou, Y., 2012. Metabolism and pharmacokinetic studies of JPH203, an L-amino acid transporter 1 (LAT1) selective compound. Drug Metab. Pharmacokinet. 27, 1, 155-161.

